Cancer Therapy & Oncology
International Journal
ISSN: 2473-554X

Juniper Publishers
key to the Researchers

Research Article
Volume 20 Issue 1 - October 2021
DOI: 10.19080/CTOIJ.2021.20.556027

Cancer Ther Oncol Int J

New Approaches of Imaging MALDI, Protein Markers Part II: Prostate Cancer Drug Targeting Chemosensitivity Biosensors

Rakesh Sharma*

Department of Radiology and Medicine, Columbia University, New York, USA

Submission: February 18, 2021; **Published:** October 25, 2021

***Corresponding author:** Rakesh Sharma, Department of Radiology and Medicine, Columbia University, New York, NY 10032, USA

Abstract

Integration of protein imaging data with tumor images and immunohistology is a new art. Identification of protein biomarkers of different cancers associated with tumorigenic pathways as 'molecular paint' is reviewed for possible correlation with tumor histology and MALDI imaging tumor characteristics in the light of recent inventions. New art of imaging MALDI is described to highlight the increased signal intensities of intracellular (IC) sodium MRI and flouro-2-deoxy-glucose utilization by PET from apoptosis protein rich MALDI visible regions of tumors "Molecular Paint" as positively correlated to chemosensitivity of Taxotere in pre- and post-taxotere treated PC-3 induced prostate explant tumors. The significance and scope of MALDI imaging, iterated protein ion mass spectrometry peak analysis is reviewed using literature data from laser raster over frozen malignant tumor slices in sequence and 3D tumor volume simulated for specific protein peak(s) distribution. A criterion of quantitative molecular painting by fusion of MRI, PET Images with MALDI and Histology was defined to evaluate malignancy by correlation, regression analysis using MRI-PET imaging, histology and MALDI imaging data from PC-3 tumor after 24 hours post-taxotere treatment. Proteomics or "protein painting" was correlated with apoptosis indices and molecule histostaining using pentachrome, feulgen and ss-DNA antibody assay. Review showed different proteins "oncoproteomics" or protein mass/electric charge (m/z) MALDI profiles measurable in tumor tissue regions signifying different features of prostate malignancy. MALDI imaging showed tumor specific protein ion species and their distribution showed empirical correlation (limited visual match) with MRI-PET signal intensities but comparable match with histology features. Recent reports strongly suggest the possibility of MRI and PET multimodal imaging integrated with MALDI-imaging as a non-invasive chemosensitivity assay to monitor the anticancer effect.

Keywords: MRI and PET integration with MALDI; Apoptosis index; Prostate tumor; Validation; MALDI imaging; Chemosensitivity

Introduction

Usually, early diagnosis of prostate cancer is difficult because of the lack of specific symptoms in early disease, poor detection limit and understanding of oncogenesis process. The "oncoproteomics" offers the identification of proteins and their interactions in a cancer cell to diagnose malignancies. Proteomics or identification of amino acids offers as tumor molecular biomarkers by matching proteins size or amino acid blots and protein array distribution in tumor. Mainly mass spectrometry (MS), reverse phase protein microarrays and 2D gel electrophoresis identify and illustrate the cancer tissue specific biomarker distribution as readable quantification format. Very recently, cancer and/ or drug action specific color-coded molecular painting methods have emerged to achieve real-time, non-invasive molecule paint arrays as proportional physio-pathochemical status of tumor cells in growing malignancy otherwise drug induced (pharmacognostic drug action) changes in structural, tumorigenic molecular density or intensity of cell cycle and/or enzyme reaction-based color change [1]. However, different physiological, physical, biochemical and energy metabolic factors inside tumor cells play a unique individual role to define the behavior and nature of intracellular tumor cells. Logistically, different imaging techniques characterize the 3D stereotactic tumor cell metabolic and molecular profile: 1. Shape and size of tumor tissues/cells, dynamics of protein NMR metabolic peaks arising from tumor cell metabolites-water contrast by Magnetic resonance imaging (MRI); 2. odd numbered atomic configuration in tumor proteins by positron emission tomography (PET) microimaging; 3. pharmaco-dynamic tumor

characterization by Matrix Assisted Laser Desorption/Ionization (MALDI) protein molecular painting or imaging-MALDI.

Author reported first time, MRI combined with Positron Emission Tomography (PET) microimaging multimodal technique to image mice prostate cancer. It recently emerged as multimodal molecular imaging tool in experimental tumor pharmaco-dynamic characterization [1]. Matrix Assisted Laser Desorption/Ionization (MALDI) based *in vivo* imaging was invented as diagnostic technique and it is emerging now as imaging multimodal MRI-PET-MALDI technique to visualize the cancer specific protein(s) for time-dependent monitoring of anticancer chemosensitivity [2]. In the direction of cancer research, sodium MRI technique is a research tool in cancer theranosis and monitoring [1]. In recent years, multimodal imaging, 3D registration-segmentation, tumor volume rendering softwares have enhanced the tumorigenic detection limit. However, MRI/PET visible tumor image tumorigenic characteristics and association with MALDI-imaging of tumor specific proteins and/or MS peak profiling remain a puzzle to correlate them with tumor physiology and histology characteristics due to difficulty of interpreting physical complexity of MRI-PET multimodal metabolic behavior, protein signal physico-chemical complexity of MALDI signal and cytomorphic complexity of histopathology structural details of tumor [2].

Time-of-flight MALDI (TOF-MALDI) is a real-time fast routine technique for accurate analysis of proteins and peptides with detail information of minute tumorigenic protein species. The mass spectroscopy detects proteins up to nanomoles based on m/z ratio by combining it with other variant mass spectroscopy SELDI, MALDI-LC, MALDI-TLC methods and modifying sample positioning, matrix composition and laser desorption/ absorption. In attempt of tumor MALDI imaging as ion distribution maps of selected m/z peaks with high intensities using Monte Carlos simulation technique, author reported to convert the MALDI peaks as points and display them as digitized simulated 'm/z' protein 'ion peak maps' at matched tumor cell locations on histology tissue sections coregistered with dynamic MRI-PET signal intensity distribution maps of tissue sodium-glucose uptake or oxygen contents [2]. These proteomic imaging techniques are of limited use to analyze protein composition as m/z peak intensities, but they offer information of tumor protein distribution. Currently, efforts are focused on integration or fusion of MRI-PET data from *in vivo* images to make gross and semi-quantitative evaluation and confirm the protein molecule alignment in tumor by integration of MALDI-histology-immunostaining data from ex vivo tissue slides to reconstruct the three-dimensional tissue volume with details of biophysico-chemical, structural and molecule makeup of tissue [1,2]. The present review focuses on chemosensitivity specific tumor biomarker mass spectrometry protein detection, physical principles of MRI-PET-MALDI fusion and quantitative proteomic MALDI imaging approach to explore the possibility of integration and fusion of in vivo and ex vivo tissue imaging-MS data.

Tumor specific Protein Biomarkers by Mass Spectrometry

Blood carcinoembryonic antigen (CEA) and HER-2 [3], human papillomavirus (HPV E6 and E7 oncoproteins) [4], CA-125, AFP fractions L3, P4/5, and the +II band [5], prostate-specific antigen (PSA) [6] are tumor markers in all solid tumors (Tables 1 & 2). The two-dimensional gel electrophoresis (2-DE) combined with matrix-assisted laser desorption/ionization time-of-flight (MALDI-TOF)/TOF MS are methods of choice to detect cancer biomarkers such as alpha-1-acid glycoprotein, clusterin down-regulation in prostate cancer, apolipoprotein A-I forms, haptoglobin alpha1, thermostable fraction by 2-DE as associated with prostate cancer malignancies. More advanced techniques are 2-D DIGE combined with nano flow liquid chromatography (LC) tandem MS, SELDI-TOF MS and PS20 chip immunoassay and Western blotting. Diagnostic oncoproteomics or tumorigenic protein (MALDI-TOF)/TOF MS profiling is useful biomarker for grading patients with prostate cancers, and benign ovarian, uterus tumors [7].

Table 1: Comparison of proteomic biomarkers and current tumor markers to highlight the better sensitivity and tumor specificity [7].

Cancer	Onco-proteomic biomarkers			Current tumor markers		
	Sensitivity	Specificity	Reference	Markers	Sensitivity	Specificity
Bladder	80%	90–97%	[5]	NMP22	31%	95%
Prostate	93%	91%	[5]	CA 15-3	63%	80–88%
Colorectal	91%	93%	[3]	CEA	43%	****
Gastric	83%	95%	[3]	CEA	49%	****
Liver	94%	86%	[5]	AFP	50%	90%
Lung	87%	80%	[5]	Cyfra21-1	63%	94%
Ovarian	83%	94%	[5]	CA-125	57%	****
Pancreatic	78%	97%	[5]	CA 19-9	72%	****

How to cite this article: Rakesh S. New Approaches of Imaging MALDI, Protein Markers Part II: Prostate Cancer Drug Targeting Chemosensitivity Biosensors. Canc Therapy & Oncol Int J. 2021; 20(1): 556027. DOI: 10.19080/CTOIJ.2021.20.556027

Table 2: *2-D DIGE combined with nano flow liquid chromatography (LC) tandem MS, SELDI-TOF MS and PS20 chip immunoassay and Western blotting (+) Overexpression of protein and (-) under-expression of protein.

Bladder cancer	Fatty acid binding proteins, annexin V, heat shock protein (Hsp) 27, and lactate dehydrogenase and less specific annexin I, 15-hydroxyprostaglandin dehydrogenase, galectin-1, lysophospholipase, and mitochondrial short-chain enoyl-coenzyme A hydratase 1 precursor proteins	squamous differentiation of the bladder transitional epithelium
Breast Cancer	lipophilin B, beta-globin, hemopexin, and vitamin D-binding protein precursor (+) Alpha2-HS-glycoprotein(-)	tumor-bearing prostates
Colorectal cancer	ANXA3, BMP4, LCN2, SPARC, MMP7, MMP11, LCN2 and MMP11(+) secretagogin(-)	Dukes stages (B,C); CRC tissues
Esophageal cancer	Periplakin, annexin V, high mobility group protein 1, C13orf2, glutamate dehydrogenase 1, fibrinogen beta chain (+) RoXaN (-)	Gastrointestinal stromal tumor
Hepatocellular carcinoma	pro-apolipoprotein, alpha2-HS glycoprotein, apolipoprotein A-IV precursor, and PRO1708/PRO2044 (the carboxy terminal fragment of albumin), leucine-rich alpha2-glycoprotein and alpha1-antitrypsin, 14-3-3γ protein (+)*; Complement C3a, ferritin light subunit, adenylate kinase 3 alpha-like 1, and biliverdin reductase B	during cell cycle regulation, apoptosis, proliferation, and differentiation
Lung cancer	5 up-regulated proteins (immunoglobulin lambda chain, transthyretin monomer, haptoglobin-alfa 2, and 2 isoforms of serum amyloid protein) (+); fragment of apolipoprotein A-I(-)	**adrenocarcinoma**
Follicular Lymphoma	histone H4 expressed protein marker	grade 1 from grade 3 follicular lymphoma
Nasopharyngeal carcinoma	ceruloplasmin	Different stages
Ovarian cancer	Hepatoglobin precursor(+) transferrin precursor (-) CA-125 levels	Different stages
Pancreatic cancer	Fibrinogen-γ, UHRF1, ATP7A, and aldehyde oxidase 1 proteins	FNAC staging
Prostate cancer	Annexin I using 2DE, Proteome Lab PF 2-D	Prostate malignancy stages
Renal cancer	Amyloid alpha protein by SEALDI	Renal malignancy
Urothelial carcinoma	Fibrinopeptide A polypeptide	Malignancy staging
Glioma	Glioma specific proteins	Grade 1 glioma
Myeloid Leukemia	Differentiation antibodies	Leukemia stages

Population Screening biomarkers for cancers

Protein diversity in population probe many protein modifications (deglycosylation, sequence truncations, side-chain residue modifications) known as Population Proteomics or tumor protein biomarker discovery [8]. For example, expression of cytokeratin (CK) 8 is positively correlated with malignancies of the head and neck areas and confirms leukoplakia with head and neck carcinoma [9].

Proteosomes in biomarker pathways define drug targets, therapeutic response monitoring and prognosis

Results from genomic and proteomic studies suggest cancer specific proteasomes in aberrant signal pathway as *biomarkers of drug targets* in a patient to fix drug targeted therapy. Proteasomes are large multi-subunit protease complexes that are localized in the nucleus and cytosol which selectively degrade intracellular proteins. They play a major role in the degradation of many proteins involved in cell cycling, proliferation, and apoptosis. For example, activation of EGFR signaling pathway in epithelial ovarian cancer can be target of cetuximab and gefitinib in clinical trial for different stages of cancer. Similarly, activation of receptor tyrosine kinases signal pathway can be target of Imatinib (c-Kit and platelet-derived growth factor receptor inhibitor), in chronic myeloid leukemia and GIST. Proteinchip® measures the kinase activity via specific detection of phosphoproteins [10]. Proteasome complex favors the proteolysis by ubiquitination of cyclin E, cyclin D, p27, IκB-α, and STAT1 in cancer tissue while docetexal induced phosphorylation of c-Fos and c-Jun, prevents their ubiquitination in cell proliferation and cell cycling processes. In fact, ubiquitin-proteasome pathway triggers the breakdown of short-lived oxidative stress and mutation proteins responsible for normal cellular homeostasis disruption. In parallel, reactive oxygen species also promote partial unfolding of these proteins, exposing its hydrophobic domains to proteolytic enzymes of 20S complex. Ubiquitin-medicated pathway in cancer also includes ubiquitin-mediated down-regulation of receptor tyrosine kinases in cancer to control of the cell cycle by the ubiquitin system and regulation of DNA repair by the ubiquitin system to initiate carcinogenesis. Constitutively, active NF-κB activation pathway is also common

How to cite this article: Rakesh S. New Approaches of Imaging MALDI, Protein Markers Part II: Prostate Cancer Drug Targeting Chemosensitivity Biosensors. Canc Therapy & Oncol Int J. 2021; 20(1): 556027. DOI: 10.19080/CTOIJ.2021.20.556027

in tumorigenesis process and proteasome inhibitor anticancer drugs block this activation to make cancer cells more susceptible to radiation therapy and chemotherapeutic agents. Following are lead examples of biomarker pathways of drug targeted cancer therapy in cancers which are evaluated by 2D electrophoresis with TOF-MALDI and coined as 'Pharmacoproteomics'

Prostate cancer

The monoclonal antibody inhibitor of HER-2, trastuzumab (Herceptin) in combination with chemotherapy slows down HER-2 over-expressing metastatic prostate cancer in women [11,12]. Proteomics-based studies have defined transforming growth factor-β-dependent regulation of cell proliferation, apoptosis, DNA damage repair and transcription to translate the transforming growth factor-β role in human prostate tumorigenesis into novel anticancer treatments and drugs in clinics [13].

Colorectal cancer

Bevacizumab and Cetuximab are first-line treatment of metastatic CRC in combination with irinotecan- or 5-FU-based chemotherapy. Bevacizumab inhibits angiogenesis by stopping interaction of VEGF with VEGFR1 (FLT-1) and VEGFR2 (KDR) on the surface of endothelial cells. Cetuximab monoclonal antibody targets the EGFR heterodimers and inhibits endogenous ligand binding by blocking receptor dimerisation, tyrosine kinase phosphorylation, and signal transduction. Cetuximab plus irinotecan and various schedule of 5-FU/FA have shown efficacy in a first-line setting [14].

Hepatocellular carcinoma

By reverse transcriptase-polymerase chain reaction, a 1,741 bp cDNA encodes a protein (HCC-2) expressed in HCC. HCC-2 is up-regulation in poor-differentiated HCC is diagnostic target for cancer therapy [15].

Prostate Cancer

Proteins expressed in prostate cancer including PSA, prostatic acid phosphatase, and prostate membrane antigens have been used as immunologic targets for immunotherapy [16].

'Pharmacoproteomics' investigates the protein expression of metabolic pathways in tumor cells to evaluate the response to anticancer agents, evaluation of radio-/chemo-therapy as optimal anticancer regimens for patients. These protein expression mechanisms mediating drug-resistance with dysregulated molecular pathways in cancer cells can profile tumor cells for selection of anticancer agents. Important to mention, are elevated urinary nuclear matrix protein NMP22 to detect recurrent bladder cancer [17]; altered cytochrome b5 and transgelin, CRABP-II, cyclophilin A, neudesin, and hemoglobin due to dysregulated cytochrome b5 dependent metabolism in progesterone receptor (PR) in estrogen receptor (ER) positive prostate cancer against tamoxifen susceptibility; high ubiquitin, low ferritin light chain in prostate cancer [18]; elevated 14-3-3σ expression in MCF7/AdVp3000 cells. Its altered expression in tumors might cause clinical resistance to chemotherapy [19]; overexpressed 3 chaperone members (Hsp27, Hsp70, and glucose-regulated protein 78) in stressful cancerous microenvironment during tumor growth and hepatocellular metastasis [19]; up-regulated HnRNPs in imatinib resistant chronic myelogenous leukemia cells due to complex Bcr-Abl activity [20]; overexpressed Hsp27 and down-regulated thioredoxin peroxidase 2 and protein disulfide isomerase proteins in non-Hodgkin's lymphoma and B cell chronic lymphocytic leukemia patients [21]; increased serum amyloid A protein isoforms, ITIH4 and PF4 markers in active disease but relapsed by salvage chemotherapy by SELDI-TOF MS, protein chip and immunoassay in nasopharyngeal carcinoma [22]; increased expression of tropomyosin family, actin family, triosephosphate isomerase family, and Hsp60, while decreased expression of enolase family proteins involved in cisplatin induced antitumor cellular energy metabolism, transformation, apoptosis, and morphologic maintenance [23]; HE4, mesothelin, M-CSF, osteopontin, kallikrein, and soluble EGF receptor serum markers in ovarian cancer [24]. Further list is growing of new protein candidates using new methods of 2-D-LC/nano-electrospray ionization-MS [25], large scale proteomic profiling by shotgun multidimensional protein identification technology (PF 2-D Proteome Lab system), offer analysis of the distribution of molecular weight, isoelectric point, and cellular localization of the eluted low abundant proteins [26]. The tandem MS-based proteomics of paraffin fixed tissues offer disease-related cancer specific biomarker concentrations.

Oncoproteomics by MRI-PET-IMS

Author proposes a new term 'Oncoproteomics' here in cancer research based on fusion of MRI-PET with MALDI imaging mass spectrometry to generate molecular map or protein painting of tumor. The discovery of new highly sensitive and specific biomarkers for early disease detection and risk stratification coupled with the development of personalized therapies is the 'oncoproteomics' to confirm metastases, invasion, and resistance to therapy as visual 3D molecular paint.

How cancer specific proteins are visualized in tissues?

MALDI Imaging Mass Spectrometry (IMS) visualizes relative abundance and spatial distribution of proteins and peptides throughout a tissue section with a lateral resolution of up to 10μm [1,2]. This technology makes use of MALDI section coated by use of a robotic matrix spotter [27]. A laser beam utilizing a grid pattern with a predefined number of laser shots per grid coordinate generates a raster of sample. IMS can also be applied to formalin-fixed and paraffin-embedded (FFPE) tissues. Now, antigen retrieval techniques coupled with *in situ* tryptic digestion permits protein analysis of FFPE samples by IMS with possible micro dissecting techniques (e.g., laser capture microdissection, LCM) [28].

How to cite this article: Rakesh S. New Approaches of Imaging MALDI, Protein Markers Part II: Prostate Cancer Drug Targeting Chemosensitivity Biosensors. Canc Therapy & Oncol Int J. 2021; 20(1): 556027. DOI: 10.19080/CTOIJ.2021.20.556027

IMS directly analyzes tissue proteins by immunohistochemistry (IHC) to measure the peptide distribution and mass/charge of protein molecules within a sample without any target specific antibody labeling reagents. IMS visualizes spatial information like histology of the tissue in imaging mode and profiling mode [29]. Profiling means small individual areas of interest are individually analyzed prior to MS analysis. For example, groups of cells (e.g., cancer and normal) can be identified on a serial section and these can be selectively analyzed. Imaging experiments measure the overall distribution of proteins as ion distribution maps of each protein signal in the mass spectra similar with histological features at high resolution.

Clinical Applications of IMS in Cancer Protein m/z Profile for Onco-proteomics

IMS studies focus on the elucidation of protein m/z differences in fresh frozen cancer tissue samples from clinical specimens of cell renal cell carcinoma (ccRCC) [30], malignant fibrous histiocytoma [31]. At distance 1.5 cm in tumor microenvironment, distribution of protein molecule changes were analyzed for under expressed tumor or adjacent tissue such as mitochondrial electron transports system; cytochrome c (*m/z* 12,272), NADH-ubiquinone oxidoreductase MLRQ subunit (*m/z* 9,368) and five cytochrome c oxidase polypeptides: subunit 5b (*m/z* 10,611); subunit 6C (*m/z* 8,577); subunit 7A2 (*m/z* 6,720); subunit 7C (*m/z* 5,354) and subunit 8A (*m/z* 4,890) in cancer ccRCC [32], non-small cell lung cancer (NSCLC) [33]. Utilizing a class-prediction model based on selected protein peaks classify tumors of different NSCLC subtypes (adenocarcinoma, squamous cell carcinoma and large cell carcinoma), primary NSCLC from lung metastases by proteomic patterns to predict nodal status and patient survival. Expression m/z protein profiles classified tumors with and without mediastinal lymph node metastasis with 85% accuracy in the training set respectively. Thus 15 peaks in a proteomic pattern indicate two small ubiquitin-related modifier-2 protein (SUMO-2) and thymosin-β4 proteins (*m/z* 10,519 and *m/z* 4,964) expression in primary NSCLC.

In other IMS study of glioma frozen sample showed proteomic patterns to predict patient survival. Combining 24 protein signals enabled patient survival by a multivariate Cox proportional hazards model for calcyclin (S100-A6, *m/z* 10,092). Dynein light chain 2 (*m/z* 10.262) protein overexpressions in STS and LTS patients. Other proteins calpactin I light chain (S100-A10, *m/z*11,073), astrocytic phosphorprotein PEA-15 (*m/z* 15,035), fatty acid-binding protein 5 (*m/z* 15,076), and tubulin-specific chaperone A (*m/z* 17,268) were overexpressed in grade IV gliomas whereas astrocytic phosphoprotein PEA-15 was predominant in grade II and III gliomas compared to grade IV gliomas [34]. HER2 receptor in fresh frozen samples by immunohistochemistry (IHC) and fluorescence *in situ* hybridization along with overexpressed cysteine-rich intestinal protein 1(CRIP1) proteins, *m/z* 8,404 in HER2 positive samples was identified [35].

Two other studies in the field of prostate cancer research reported the identification of proteomic markers that predict treatment response in prostate cancer. Samples from prostate cancer patients receiving a neoadjuvant therapeutic treatment regime with paclitaxel and radiation were analyzed by histology directed profiling and gene expression profiling [36]. From a total of 38 patients enrolled in this study, fresh frozen samples from 19 patients were available to perform IMS analysis. After treatment, 6 patients showed a pathological complete response and 13 were determined as non-responders' due presence of residual disease. Three highly overexpressed (>30-fold) features (*m/z* 3,371, *m/z* 3,442 and *m/z* 3,485) and four features of lower expression (*m/z* 5,667, *m/z* 6,955, *m/z* 7,007 and *m/z* 15,348) were revealed in the responder group by spectral comparison between tumor regions from both groups. As previously identified by other research groups, the three overexpressed features represent defensins (*m/z* 3,371, α-DEFA1; *m/z*3,442, α-DEFA2 and *m/z* 3,485, α-DEFA3). These cytotoxic peptides are primarily known to be abundant in neutrophils. IHC was performed to elucidate the source of DEFA expression and obviate a false positive result due to blood contamination of the samples. IHC results verified that besides infiltrating neutrophils, the tumor cells showed a positive staining for DEFA in patients with a pathological complete response whereas non-responders exhibited little or no staining of the tumor cells. DEFA was not found to be overexpressed in the gene expression profiling studies that only revealed genes from immune response categories to be differentially expressed. These results highlight the independent value of proteomic based approaches and its importance in discovery of protein differences at the posttranslational level that cannot be identified at the genomic level.

An earlier study of mammary tumors in mouse mammary tumor virus/HER2 transgenic mice was able to predict treatment response to a small molecule inhibitor of the epidermal growth factor receptor tyrosine kinase (elortinib) and/or a HER2 blocking antibody (trastuzumab) by assessing early proteomic changes directly in the tumor by IMS [37]. Fresh frozen tumor sections at various time points after drug administration were compared to sections from untreated mice. Time- and dose-dependent related proteomic changes were observed. Elortinib treatment induced a decrease in thymosin beta-4 (*m/z* 4,965) as well as ubiquitin (*m/z* 8,565) and an increase of a fragment of E-cadherin binding protein (*m/z* 4,794) in tumor sections when compared to tumors from untreated mice. Even bigger changes in thymosin beta 4 and the fragment of E-cadherin binding protein were noticed when a combinational treatment with both drugs was administered. This combinational treatment resulted in an additional proteomic change not observed in the single dosed tumors; a calmodulin fragment (*m/z* 8,719) was found to be increased considerably. Additional proteins found to be upregulated in tumors treated with both drugs include ubiquitin, acyl-CoA binding protein, calgizzarin, histone H3 and histone H4. Spatial distribution studies of elortinib obtained directly from tissue sections by IMS also correlated with these proteomic changes, thus emphasizing the strength and versatility of IMS.

How to cite this article: Rakesh S. New Approaches of Imaging MALDI, Protein Markers Part II: Prostate Cancer Drug Targeting Chemosensitivity Biosensors. Canc Therapy & Oncol Int J. 2021; 20(1): 556027. DOI: 10.19080/CTOIJ.2021.20.556027

Studies of prostate cancer have utilized IMS to aid in the diagnosis of this highly prevalent disease and to discover proteins relevant to the underlying biology [38]. In one study, investigators compared 31 fresh frozen prostate cancer and 41 normal prostate biopsies with the aim to identify peptides differentially expressed between both groups [38]. Two peptides (*m/z*4,027 and *m/z* 4,355) showed significant overexpression in cancer samples whereas m/z 4,274 was predominant in benign areas. For statistical analyses, the sample set was divided in a discovery set (cancer, n=11; normal, n=10) and an independent validation set (cancer, n=23; normal, n=31). A correct classification of 85% and 81% in the discovery set and validation set, respectively, was achieved by combining the three peptides in a genetic algorithm-based model. The peptide at *m/z* 4,355, overexpressed in cancer tissue, was identified as a fragment of mitogen-activated protein kinase/extracellular signal-regulated kinase kinase kinase 2 (MEKK2). Expression of this fragment could be shown to decrease with increasing Gleason grade and a significant reduction could be observed between pathological stage pT2 and pT3b. MEKK2 overexpression could further be validated by Western blot analysis and IHC, both of which found MEKK2 overexpressed in prostate cancer tissue and prostate cancer cell lines.

In a similar study of ovarian cancer, fresh frozen ovarian cancer tissue samples (n=25) were analyzed in comparison to benign ovarian tumors (n=23) [39]. A putative marker for ovarian cancer was detected at *m/z* 9,744 with a prevalence of 80%. This feature was identified as a fragment of the 11S proteasome activator complex, Reg-alpha (m/z 9,744). Validation of IMS results was performed by Western blot analysis as well as IHC. The Western blot showed a detection of the complete protein (28 kDa) in 6 of 9 carcinoma samples whereas 3 out of 16 benign tumors showed a slightly positive result. The latter revealed distinct and diagnosis dependent localization within cellular compartments with cytoplasmatic localization of Reg-alpha in carcinomas and no cytoplasmatic but nuclear staining in 76.9% of benign tumors. Other studies of oral squamous cell carcinoma [40], tumor interfaces in ovarian cancer [41], meningioma progression [3] and classical Hodgkin lymphoma [42] also show the capabilities of IMS in these types of applications.

Peptide Analysis and IMS: Protein Molecular Painting in clinical studies

Formalin-fixed and paraffin-embedded clinical specimens IMS analysis is advanced technology. Analysis of FFPE tissue is done by combining heat induced antigen retrieval techniques and enzymatic sample digestion [43]. Tryptic digestion also allows analysis of high molecular weight proteins. A study of FFPE tissue microarray (TMA) samples from NSCLC tissues established IMS technology as a high-throughput platform for the classification of subtypes of NSCLC [28] combing 73 peaks in a support vector machine algorithm-based model to enable the correct classification of all patients. TMA by MALDI MS/MS analysis showed three tryptic peptides (*m/z* 987.60; *m/z*1163.62 and *m/z* 1905.99) originating from heat shock protein beta-1 and other peptide (*m/z* 1410.70), identified as a tryptic peptide from keratin type II cytoskeletal 5 in squamous cell carcinomas.

A classic study on FFPE tissue samples from pancreatic adenocarcinoma samples using MALDI ion mobility MS showed identification of tryptic peptides [44]. For example, squamous cell carcinoma samples of the lung and skin showed protein *m/z* 1891.3 and *m/z* 1829.2 in the hippocampus identified by tandem MS as a tryptic peptide of tubulin beta-4 chain.

IMS analysis in drug Induced Changes

IMS analysis was employed to assess the drug metabolism and drug induced changes to proteins by tandem mass spectrometry (MS/MS) [45]. Localization of oxaliplatin and its derivates by IMS [46]. Vinblastine distribution within different organs were imaged by IMS (precursor ion *m/z* 811.4) and its fragments (e.g. m/z 793) in the liver, kidney and tissue surrounding the gastrointestinal tract [47]. The distribution of epidermal growth factor receptor inhibitor (erlotinib) and its metabolites was analyzed by IMS in tissue sections [48]. However, quantitative analysis of the drug by MALDI MS with standard liquid chromatography tandem MS analysis (LC-MS/MS) gives similar ratios of total ion intensities from liver and spleen homogenate samples. In imaging MALDI fusion experiments, software tools identify signals from specific tumor features which generate digital stained images of tumor by unsupervised or supervised classification algorithms [49]. For fusion, reconstructed three-dimensional (3D) volumes are generated utilizing virtual z-stacks and 3D volume rendering tools. These IMS based data is co-registered with block face optical images and MRI-PET data [1,2, 50,51]. Such protein and peptide analysis offers: 1. diagnostic comparison of different tissue types (e.g., tumor versus normal); 2. prognostic studies to differentiate patients with long- or short-term survival; and 3. drug response predicting a patient's response to a certain treatment.

A new fusion art of Imaging MALDI with MRI-PET and Immunostaining

Fusion of tumor protein (proteomics by MALDI) and MRI-PET imaging is described in detail by author in experimental tumor analysis [1]. The principle of fusion is since protons act as coin with two faces (one sensitive to MALDI and other sensitive to MRI-PET). MALDI imaging is protein specific to metabolic disorder in various prostate malignant tumor stages. Same time, protons in tumor protein molecules and glucose-oxygen in tumor generate composite m/z spectra with color coded molecule paint in box format (see Figure 1). Pixel-by-pixel transversion converts MRI-PET image dots appearing as 3D box originated from superimposition of MRI slices with dynamic PET pixels (see Figure 2) and point co-ordinates on MALDI rasters from different tumor slides using Monte-Carlos's simulations (see Figure 3).

How to cite this article: Rakesh S. New Approaches of Imaging MALDI, Protein Markers Part II: Prostate Cancer Drug Targeting Chemosensitivity Biosensors. Canc Therapy & Oncol Int J. 2021; 20(1): 556027. DOI: 10.19080/CTOIJ.2021.20.556027

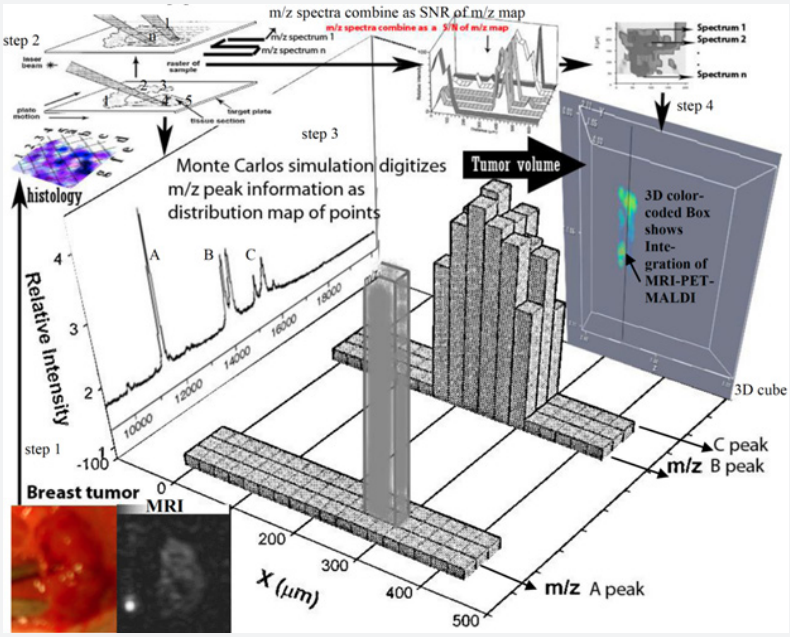

Figure 1: Outline of MALDI-MRI-PET-immunostaining integration of digital tumor images is shown to generate a MALDI map of proteins to highlight the m/z peak selection and peak digitization to reconstruct proteomics map and 3D tumor volume. After MRI-PET imaging, tumor is excised and processed for histology and MALDI to generate a rasterized information of tumor cytometry (shown as 1-5 and a to g regions) with corresponding (spectra 1,2.. n) of protein distribution in prostate tumor tissue. Note the spatial information of protein ions in 3D cube on right obtained by thresholding and baseline correction. The 3D tumor digital information is fused with MRI-PET images. See Figure (4) for better visualization. Modified from reference [1].

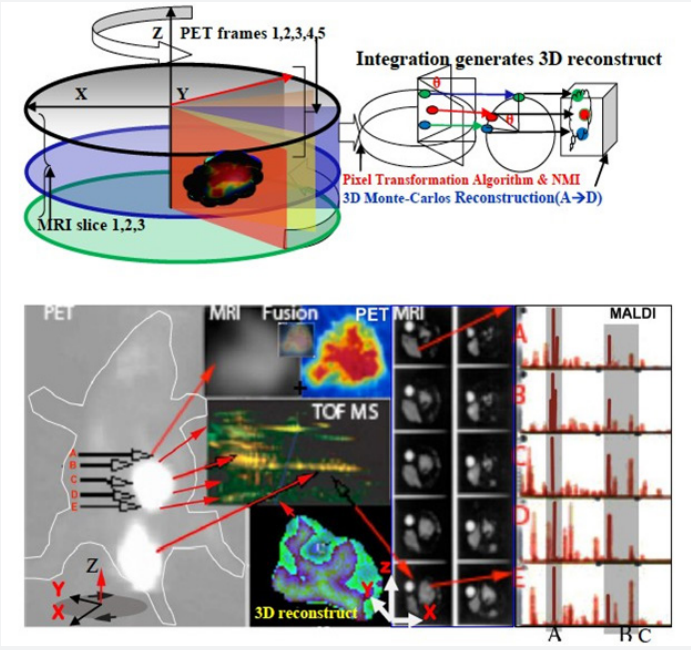

Figure 2: (top panel) MRI-PET-MALDI data integration method is sketched. (Bottom panel) A rat prostate tumor (PET image on left) after taxotere treatment is shown. First row (in middle at top) with MRI-PET image fusion at different MRI slice levels (second column in right). Notice the high color-coded signal intensities of tumor provides the taxotere effect while same tissue locations show specific TOF-MALDI peaks as finger print of taxotere effect (second raw in middle) and Monte-Carlos simulated 3D tumor reconstructed volume as display of 3D protein map in registration with MRI-PET piled up slice volume of shrunk tumor size (at bottom panel in middle). The detailed protein distribution (on bottom panel at right) with MS-MALDI peaks provide peptide informatics or tumorigenic protein 3D makeup (peaks A and B shown in tumor locations A-E) in the tumor volume. Modified from reference [1].

How to cite this article: Rakesh S. New Approaches of Imaging MALDI, Protein Markers Part II: Prostate Cancer Drug Targeting Chemosensitivity Biosensors. Canc Therapy & Oncol Int J. 2021; 20(1): 556027. DOI: 10.19080/CTOIJ.2021.20.556027

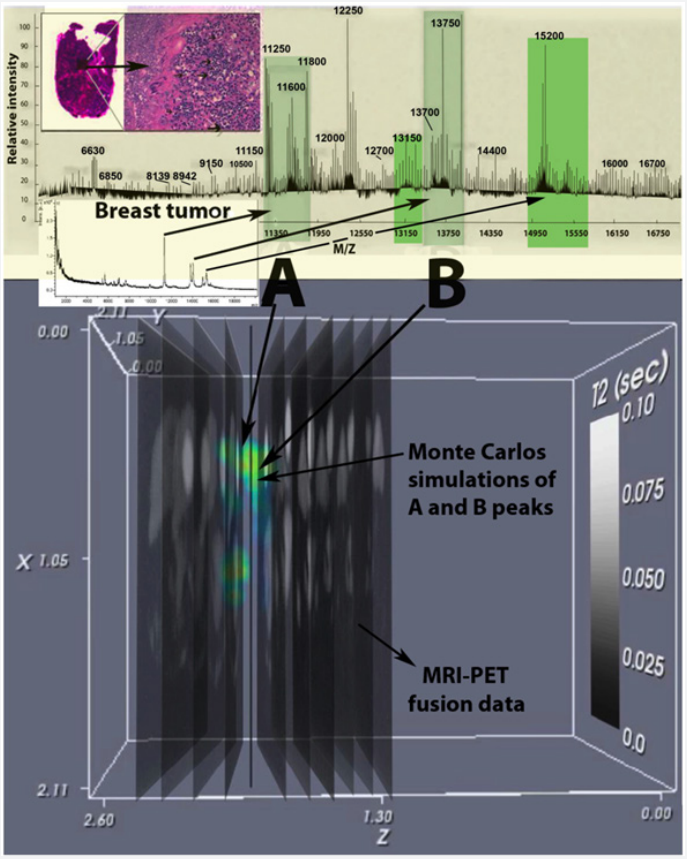

Figure 3: (on top row) A tumor histology section with high power microscopy area (see arrows for apoptosis) is shown with corresponding MALDI optimized peaks A and B. The peaks A and B were digitized by Monte Carlo simulation (A and B shown with arrows) and integrated with MRI-PET images to generate a 3-dimensional tissue reconstruct. The tumor proteomics-image volume was used to compare chemosensitivity. Modified from reference [1].

Discussion

Proteosomes are smart cancer biomarker proteins detectable by MALDI as tumor stage specific protein m/e values. These biomarker proteins play significant role in regulation of specific metabolic pathways at various stages so are used to track and predict the tumorigenic changes in tumor. Based on biomarker protein mass spectrometry peaks, metabolite distribution can be visualized as 'molecular paints. Several new terms are proposed such as onco-proteomics, imaging theraproteomics, oncoprotein profiles. In addition, the integrated MRI-PET-MALDI data pixel-by-pixel fusion with protein m/z distribution facilitates to explore apoptotic protein(s) as shown in Figure 2. The proteomics information of PC-3 cells is well documented by MALDI MS spectroscopy and PEG electrophoresis to identify potential protein biomarkers to predict response to chemotherapy in cancer [1,2]. Status of MALDI imaging as adjunct remains disputed because of several artifacts including low intrinsic abundance, inefficient ionization, and/or signal suppression of most common peptides may limit or even prevent detection, unless the apoptosis sensitive phosphopeptide(s) content is significantly enriched by electrophoresis prior to MALDI analysis.

MALDI peaks (m/z with 11250(A), 13750(B) Da and m/z with 13700 and 15200(C) Da small peaks with three major peaks (m/z with 6,630, 8,139 and 8,942 Da) are shown in Figure 3 for prostate tumor data set. The proteomics analysis identifies and characterizes tumor-associated protein variants associated with apoptosis by two-dimensional electrophoresis and MALDI mass spectrometry. Several tumor apoptosis-associated variants AKR1C1 or -C3, AKR1B1 represent the proteins of the aldo-keto reductase superfamily; aldose reductase-like protein-1 (rARLP-1) (69% sequence identity to lens aldose reductase) and three additional types of rARLP-1; and aldo-keto reductase protein-c (Rak-c), a novel tumor-associated variant (65% sequence identity with 3a-hydroxysteroid dehydrogenase); reduced 3a-hydroxysteroid dehydrogenase and 4y -3-ketosteroid-5α-reductase enzymes in prostate tumors. The coregistration of 3D co-ordinates on MRI/PET and histology digital images offers composite information of tumor protein molecular details.

How to cite this article: Rakesh S. New Approaches of Imaging MALDI, Protein Markers Part II: Prostate Cancer Drug Targeting Chemosensitivity Biosensors. Canc Therapy & Oncol Int J. 2021; 20(1): 556027. DOI: 10.19080/CTOIJ.2021.20.556027

The real time monitoring of docetaxal (Taxotere) drug chemosenstivity effect for 0-48 hours was reported in terms of shrunken tumor mass by sodium MRI and decrease in hyperglycolytic tumor tissue with possible MALDI-IMS visible premalignancy or malignancy specific tumor protein(s) [1]. Identification of major carcinogenic responsible tumor proteins is a challenge because MALDI peaks are showing m/z peaks of proteins or peptides from a very small tumor region (difficult to take away specimen from big mass of tumor) while PEG electrophoresis protein/peptide map shows presence of tumor proteins (with different pI) in large number without any confirmation of responsible tumorgenic or apoptotic or premalignant protein(s).

Other important issue was how spatial and quantitative information from proteomics may extend the protein predictability from in vivo MALDI-IMS studies to test drug action or to predict functional regulatory protein information responsible of tumor apoptosis and angiogenesis (proteomics profiling), signaling mechanism and molecular mechanism of programmed tissue degradation (protein expression) and cancer protein mapping. The spatial distribution of tumor cell protein molecules as false color 'molecular paints or maps can open window to the visible biochemical changes with insight of biophysical basis of MRI image contrast and physiological basis of PET contrast [51].

Current and future Developments

Functional imaging, biosensors, and sophisticated computational biology are having an unprecedented impact on the cancer detection and oncopharmaceutical industry. Advanced proteomic platforms such as Orbitrap MS, Fourier transform ion cyclotron resonance MS, and protein microarrays can generate a rapid and high-resolution portrait of the proteome. Emerging novel nanotechnology strategies to amplify and harvest tumor biomarkers *in vitro* or *in vivo* will greatly enhance our ability to discover and characterize molecules for early cancer detection, subclassification, and prognostic capability of current proteomic modalities. New types of proteomic technologies combined with advanced bioinformatics are currently being used to identify molecular signatures of individual tumors based on protein pathways and signaling cascades. It is envisaged that analyzing the cellular circuitry of ongoing molecular networks will become a powerful clinical tool in cancer patient management. Analysis of tumor-specific proteomic profiles permits better understanding of neoplasia development and the discovery of novel molecular targets for cancer therapy.

Recently several inventions and patents have suggested the possibility of multimodal imaging by integrating digital data from morphometric imaging with molecular imaging such as MALDI, immunostaining. The Previously, author showed the distribution of 18-FDG-PET and sodium MRI signal intensities in tumor as measurable and diagnostic by imaging methods [1,2]. There are three main approaches of PET/MRI integration architecture: sequential, insert and integrated types. Major challenges are: 1. Potential cross talk effects in front-end electronics due to fluctuations in light yield of scientillators in PET detectors caused by rapidly changing MR gradients and RF signals; 2. Magnetic inhomogeneities; 3. Compensation of Eddy currents and better shimming; 4. Better PET attenuation- scatter-random coincidence correction algorithms; 5. Detector technology with matching scintillation crystals combined with less sensitive light sensors. In future new technology of magnetic field insensitive avalanche photodiodes, design shielded PET electronics will be available to avoid electromagnetic interference. In future, quantitative MRI- PET-MALDI-histoimmunostaining criterion can or will distinguish apoptosis-rich and benign or malignant tumor features for theranosis. Sodium MRI and PET image intensities is a new information showing positive correlation with histology and apoptosis premalignancy proteomics indices as rapid drug monitoring time-dependent assay. In this direction, recently inventors modified and suggested design of transparent MALDI slides, antibody-peptide conjugate mediated MALDI imaging by fast fragmentation method and new thresholding techniques of MALDI peak selection. 3D digital mapping of MALDI is in infancy.

Specimen manipulations such as sample collection, pipetting, and diluting also contribute to pre-analytical variables for discovery (training) sets and validation (testing) sets. Differences in sample collection, handling or storage, and profiling techniques, may influence the protein profile obtained from a given sample. Standardization of techniques, proteome analyses in the clinical setting, cost are precluding factor for the widespread use of proteomics in clinical laboratory. Another major challenge is the integration of proteomic with genomic and metabolomic data and their functional interpretation in conjunction with clinical results and epidemiology.

In near future, proteomic technology with huge datasets with more than a million variables will pose difficulties. Usual approach using simple ANOVA approach is not sufficient. It not only neglects correlations between variables, but silent on discriminatory information. Different approaches are necessary and multivariate analysis should become a standard one. The stable isotope standards and capture ELISA assay by anti-peptide antibodies and multiple-reaction-monitoring MS may be suitable as multiplexed assays for several potential biomarkers. In future, technical advancements may accomplish the purpose of quantitative noninvasive MALDI imaging combined with multinuclear in vivo proton- intracellular sodium and glycolysis imaging indicators of tumorigenesis (apoptosis, necrosis, proliferation, premalignancy or malignancy) to test anticancer drug chemosensitivity. It remains to see the new inventions how advanced techniques solve the problem of integrating in vivo imaging data with ex vivo molecular imaging data to construct three-dimension tumor volume of molecular details

How to cite this article: Rakesh S. New Approaches of Imaging MALDI, Protein Markers Part II: Prostate Cancer Drug Targeting Chemosensitivity Biosensors. Canc Therapy & Oncol Int J. 2021; 20(1): 556027. DOI: 10.19080/CTOIJ.2021.20.556027

or IMAGING THERAPROTEOMICS (molecular painting) to test anticancer drug effects. Cancer specific proteins will have a significant impact on the development of future diagnostic and therapeutic products. In years to come, a serum or urine test for every phase of cancer may drive clinical decision making, supplementing or replacing currently existing invasive techniques.

Conclusion

The proteasomes as cancer smart biomarker protein profiles by MALDI imaging and possible MRI-PET data integration is explored and reviewed with a focus on the progress of quantitative MRI-PET and MALDI protein detection applications to test anticancer drug. Review of initial trials and patents showed the approach of integrated MRI/PET imaging and immunostaining, histology and MALDI data may construct 'metabolic paints' to show cancer specific protein distribution and correlation as sensitive, tumor specific, accurate reproducible and precise to define tumorigenic cancer stages in theranosis of tumors.

Acknowledgement

This manuscript in part was presented at peer-reviewed AFLAC award at AACR meet 2002, ISMRM workshop 2001 and ISMRM annual meet 2002. MALDI-IMS data was presented by Doris Terry at ASMS 2007. The authors wish to acknowledge the experimental data and expertise provided by Drs. Ed X. Wu, Paul Cannon, van Heertum, Kenny Hess at Radiology department and Dr. Matthias Schbolcs and Dr. Mansukhani at Pathology department and helping in these imaging and continuing tumor histology experiments. Authors wish to acknowledge the MALDI-IMS and peak analysis done by Dr. Doris Terry at Florida State University, Tallahassee, Florida. Grant source: Aventis Pharmaceuticals Company, Bridge-water, NJ. Figures were improved by Mr. Magesh Sadasivam at Amity Institute of Nanotechnology, Amity University UP, NOIDA, India.

Conflict of Interest

Authors do not have any financial or commercial conflict.

Appendix 1

Sample preparation protocols are common for both imaging and protein profiling. For fresh frozen tissue samples, ~5–20 µm thick sections are cut on a cryostat and thaw mounted on a metal target or conductive glass slide. For protein analysis, excess lipids and salts can interfere with matrix crystallization and analyte ionization, therefore sections are typically fixed with graded ethanol washes (70%, 90%, 95% for 30 sec each). This established histology procedure also ensures sample dehydration and fixation of the proteins while maintaining the tissue architecture. Some histological stains such as hematoxylin and eosin (H&E) interfere with subsequent MS analyses, thus serial sections are often obtained and stained to guide matrix deposition and laser ablation (ie, in a histology-directed profiling experiment) and to allow comparison of MS results with tissue histology.

H&E staining of the same section involves first performing MS analysis followed by matrix removal and subsequent counterstaining. Several classes of proteins such as integral membrane proteins or hydrophobic proteins require sample pretreatment protocols [52]. Application of matrix in a MALDI MS experiment for protein analysis (molecular weight > 2 kDa) needs sinapinic acid (SA), for peptides (molecular weight 500–3000 Da) α-cyano-4-hydroxycinnamic acid (CHCA), and for small molecules such as lipids and drugs, 2,5-dihydroxybenzoic acid (DHB). The matrix is typically dissolved in a solvent solution of 50% acetonitrile with 0.1% trifluoroacetic acid [53].

Manual application of ~250 nL – 1 µL matrix solution is used for large matrix spots (~0.5–1 mm in diameter). Robotic spotting devices also used to place small matrix spots depositing 50–100 pL volumes at specific x, y coordinates on tissue sections for protein profiling [54]. Multiple passes of matrix application are required to achieve optimal analyte extraction and matrix crystallization. Matrix application for imaging experiments is performed by either applying the matrix in an ordered array of dense matrix spots using robotic devices.

FFPE tissue samples are cut at 5 µm using a microtome and mounted onto conductive targets. After paraffin removal in xylene and graded ethanol washes, immunohistochemistry protocols are followed. Sections are antigen retrieved, typically by incubating the section in a heated buffer solution (e.g. citrate or tris buffer) for 20 min. Subsequently, on-tissue enzymatic digestion is performed, usually by robotically spotting enzyme solution on the tissue in the same manner as that described above for matrix application [28]. After digestion, matrix is applied to these spots; and the tissue is analyzed. Data is acquired for both profiling and imaging similarly by moving the sample stage under a fixed laser focus position. At each x, y position, multiple laser shots are summed to generate a single spectrum for that given position. For protein analyses, mass spectra are typically acquired in a mass range from 2–50 kDa.

Mass spectral processing steps include baseline subtraction, noise reduction, mass calibration and normalization to total ion current (TIC) of each spectrum. Features of interest detected peak areas or intensities that meet certain threshold criteria (ie, minimal S/N, prevalence in certain percentage of sampled spectra) can be subjected to statistical analysis. Specific algorithms combine multiple spectral features in a model that distinguish spectra from each group.

How to cite this article: Rakesh S. New Approaches of Imaging MALDI, Protein Markers Part II: Prostate Cancer Drug Targeting Chemosensitivity Biosensors. Canc Therapy & Oncol Int J. 2021; 20(1): 556027. DOI: 10.19080/CTOIJ.2021.20.556027

MRI-PET-MALDI Registration

The static deformed PET registration with slice-by-slice MRI sections to demonstrate the point-wise match between MRI-PET signal intensities and protein MALDI peaks or images. A 'quantitative MRI- PET-MALDI criterion' was developed to validate and correlate the MRI/PET microimaging for tumor intracellular sodium signal intensities and PET active hyper-glycolytic regions, with MALDI protein peaks and histology tumor features [1,2]. The assumptions of tumor cells were: 1. Loss of membrane sodium pump/symporter is associated with glucose pump and loss of oxygen (low oxidative phosphorylation makes high glycolysis); 2. In tumorigenesis, low oxidative phosphorylation, high glycolysis, apoptosis, necrosis, cell proliferation, cell death occurs in a sequence; 3. The events of tumorigenesis or drug antitumor action are detectable by in vivo oxidative phosphorylation and intracellular sodium (by MRI), in vivo high glycolysis and oxygen (by PET), apoptosis proteins (by MALDI protein peaks), ex vivo cytomorphometric changes of apoptosis, proliferation, necrosis, cysts (by histology); 3. Multimodal hybrid molecular imaging provides a finger print of tumorigenic kinetics and antitumor pharmacokinetics or therapeutic monitoring (Quantitative Theranosis).

Technique Development for MALDI-IMS Data Acquisition

Mass spectrometer was tuned and controlled in its operations for TOF-MALDI MS spectroscopy mode, and it was also used as the data source to acquire, process, store, and print. Most of the analog electrical signals reach the computer after analog-to-digital converter is used. In reverse order, digital signal can be converted to analog signal. However, in MALDI, transputer is used as digital device to convert its electrical signals in the form of pulses or proportional m/z peak intensities. A mass spectrum has m/z values (peaks) each showing peak height proportional to number of protein ions with unit charge. The m/z peak shapes from selected tumor tissue locations on MALDI slide (protein molecules) generate a set of electrical signals at preset voltage (checking is important in different Scanning modes). By manipulation of mass spectra data, accurate mass measurement was done (relevant peak sorting by thresholding at a certain peak height) to gather important m/z peaks and compare with calibrated reference peaks of reference CHACA and HABA calibrated compounds. By 'match and try' a set of peptides was selected to determine the protein make-up (proteomics finger print) using MOSCOT and Swiss library search for molecule identification as shown in Figure 1 at the bottom.

Tumor tissue samples were prepared for MALDI data using techniques described in a previous study [1]. Collected tissue sections were transferred using rice paper to gold coated MALDI target plates (Applied Biosystems Inc.) and spray-coated with a 25 mg/mL sinapinic acid matrix solution prepared in 60% acetonitrile, 0.5% trifluoroacetic acid. Approximately 10 mL of matrix solution were needed to produce a homogeneous matrix crystal layer. Matrix coated samples were then analyzed on a linear MALDI-time-of-flight mass spectrometer (Autoflex II, Bruker Daltonics Inc.) equipped with a Smartbeam™ laser.

References

1. Sharma R, katz JK (2011) Taxotere Chemosensitivity Evaluation in Rat Prostate Tumor by Multimodal Imaging: Quantitative Measurement by Fusion of MRI, PET Imaging with MALDI and Histology. Recent Patents on Medical Imaging 1(2).
2. Sharma R, Katz JK (2008) Taxotere chemosensitivity evaluation in mice prostate tumor: Validation and diagnostic accuracy of quantitative measurement of tumor characteristics by MRI, PET and histology of mice tumor. Technol Cancer Res Treat 7(3): 175-185.
3. Agar NY, Malcolm JG, Mohan V, Yang HW, Johnson MD, et al. (2010) Imaging of Meningioma Progression by Matrix-Assisted Laser Desorption Ionization Time-of-Flight Mass Spectrometry. Anal Chem 82(7): 2621-2625.
4. Andersson M, Groseclose MR, Deutch AY, Caprioli RM (2008) Imaging mass spectrometry of proteins and peptides: 3D volume reconstruction. Nat Methods 5(1): 101–108.
5. Bauer JA, Chakravarthy AB, Rosenbluth JM, Mi D, Seeley EH, et al. (2010) Identification of markers of taxane sensitivity using proteomic and genomic analyses of prostate tumors from patients receiving neoadjuvant paclitaxel and radiation. Clin Cancer Res 16(2): 681–690.
6. Becker KF, Schott C, Hipp S, Metzger V, Porschewski P, Beck R, et al. (2007) Quantitative protein analysis from formalin-fixed tissues: implications for translational clinical research and nanoscale molecular diagnosis. J Pathol 211(3): 370–378.
7. Bouslimani A, Bec N, Glueckmann M, Hirtz C, Larroque C (2010) Matrix-assisted laser desorption/ionization imaging mass spectrometry of oxaliplatin derivatives in heated intraoperative chemotherapy (HIPEC)-like treated rat kidney. Rapid Commun Mass Spectrom 24(4): 415-421.
8. Herring KD, Oppenheimer SR, Caprioli RM (2007) Direct tissue analysis by matrix-assisted laser desorption ionization mass spectrometry: application to kidney biology. Semin Nephrol 27(6): 597–608.
9. Kang S, Shim HS, Lee JS, Kim DS, Kim HY, et al. (2010) Molecular proteomics imaging of tumor interfaces by mass spectrometry. J Proteome Res 9(2): 1157–1164.
10. Rauser S, Marquardt C, Balluff B, Deininger SO, Albers C, et al. (2010) Classification of HER2 Receptor Status in Prostate Cancer Tissues by MALDI Imaging Mass Spectrometry. J Proteome Res 9(4): 1854-1863.
11. Ronci M, Bonanno E, Colantoni A, Pieroni L, Di Ilio C, et al. (2008) Protein unlocking procedures of formalin-fixed paraffin-embedded tissues: application to MALDI-TOF imaging MS investigations. Proteomics 8(18): 3702–3714.
12. Schiller J, Suss R, Arnhold J, Fuchs B, Lessig J, et al. (2004) Matrix-assisted laser desorption and ionization time-of-flight (MALDI-TOF) mass spectrometry in lipid and phospholipid research. Prog Lipid Res 43(5): 449-488.
13. Schwamborn K, Krieg R, Jirak P, Ott G, Knuchel R, et al. (2010) Application of MALDI imaging for the diagnosis of classical Hodgkin lymphoma. J Cancer Res Clin Oncol 136(11): 1651-1655.

How to cite this article: Rakesh S. New Approaches of Imaging MALDI, Protein Markers Part II: Prostate Cancer Drug Targeting Chemosensitivity Biosensors. Canc Therapy & Oncol Int J. 2021; 20(1): 556027. DOI: 10.19080/CTOIJ.2021.20.556027

14. Schwamborn K, Krieg RC, Reska M, Jakse G, Knuechel R, et al. (2007) Identifying prostate carcinoma by MALDI-Imaging. Int J Mol Med 20(2): 155–159.

15. Schwartz SA, Reyzer ML, Caprioli RM (2003) Direct tissue analysis using matrix-assisted laser desorption/ionization mass spectrometry: practical aspects of sample preparation. J Mass Spectrom 38(7): 699–708.

16. Schwartz SA, Weil RJ, Thompson RC, Shyr Y, Moore JH, et al. (2005) Proteomic-based prognosis of brain tumor patients using direct-tissue matrix-assisted laser desorption ionization mass spectrometry. Cancer Res 65(17): 7674–7681.

17. Sinha TK, Khatib-Shahidi S, Yankeelov TE, Mapara K, Ehtesham M, et al. (2008) Integrating spatially resolved three-dimensional MALDI IMS with in vivo magnetic resonance imaging. Nat Meth 5(1): 57–59.

18. Sloane AJ, Duff JL, Wilson NL, Gandhi PS, Hill CJ, et al. (2002) High throughput peptide mass fingerprinting and protein macroarray analysis using chemical printing strategies. Mol Cell Proteomics 1(7): 490–499.

19. Tost J, Gut IG (2006) DNA analysis by mass spectrometry-past, present and future. J Mass Spectrom 41(8): 981–995.

20. Trim PJ, Henson CM, Avery JL, McEwen A, Snel MF, et al. (2008) Matrix-assisted laser desorption/ionization-ion mobility separation-mass spectrometry imaging of vinblastine in whole body tissue sections. Anal Chem 80(22): 8628–8634.

21. Wagner M, Varesio E, Hopfgartner G (2008) Ultra-fast quantitation of saquinavir in human plasma by matrix-assisted laser desorption/ionization and selected reaction monitoring mode detection. Journal of Chromatography B 872(1-2): 68–76.

22. Walch A, Rauser S, Deininger SO, Hofler H (2008) MALDI imaging mass spectrometry for direct tissue analysis: a new frontier for molecular histology. Histochem Cell Biol 130(3): 421–434.

23. Wilson KS, Roberts H, Leek R, Harris AL, Geradts J (2002) Differential gene expression patterns in HER2/neu-positive and -negative prostate cancer cell lines and tissues. Am J Pathol 161(4): 1171–1185.

24. Wisztorski M, Franck J, Salzet M, Fournier I (2010) MALDI direct analysis and imaging of frozen versus FFPE tissues: what strategy for which sample? Methods Mol Biol 656: 303–322.

25. Xu H, Yang L, Wang W, Shi SR, Liu C, et al. (2008) Antigen retrieval for proteomic characterization of formalin-fixed and paraffin-embedded tissues. J Proteome Res 7(3): 1098–1108.

26. Yanagisawa K, Shyr Y, Xu BJ, Massion PP, Larsen PH, et al. (2003) Proteomic patterns of tumour subsets in non-small-cell lung cancer. Lancet 362(9382): 433–439.

27. Chaurand P, Schwartz SA, Reyzer ML, Caprioli RM (2005) Imaging mass spectrometry: principles and potentials. Toxicol Pathol 33(1): 92–101.

28. Groseclose MR, Massion PP, Chaurand P, Caprioli RM (2008) High-throughput proteomic analysis of formalin-fixed paraffin-embedded tissue microarrays using MALDI imaging mass spectrometry. Proteomics 8(18): 3715–3724.

29. Cornett DS, Reyzer ML, Chaurand P, Caprioli RM (2007) MALDI imaging mass spectrometry: molecular snapshots of biochemical systems. Nat Methods 4(10): 828–833.

30. Herring KD, Oppenheimer SR, Caprioli RM (2007) Direct tissue analysis by matrix-assisted laser desorption ionization mass spectrometry: application to kidney biology. Semin Nephrol 27(6): 597–608.

31. Caldwell RL, Gonzalez A, Oppenheimer SR, Schwartz HS, Caprioli RM (2006) Molecular assessment of the tumor protein microenvironment using imaging mass spectrometry. Cancer Genomics and Proteomics 3: 279–288.

32. Oppenheimer SR, Mi D, Sanders M, Caprioli RM (2010) A Molecular Analysis of Tumor Margins by MALDI Mass Spectrometry in Renal Carcinoma. J Proteome Res 9(5): 2182-2190.

33. Yanagisawa K, Shyr Y, Xu BJ, Massion PP, Larsen PH, et al. (2003) Proteomic patterns of tumour subsets in non-small-cell lung cancer. Lancet 362(9382): 433–439.

34. Schwartz SA, Weil RJ, Thompson RC, Shyr Y, Moore JH, et al. (2005) Proteomic-based prognosis of brain tumor patients using direct-tissue matrix-assisted laser desorption ionization mass spectrometry. Cancer Res 65(17): 7674–7681.

35. Rauser S, Marquardt C, Balluff B, Deininger SO, Albers C, et al. (2010) Classification of HER2 Receptor Status in Prostate Cancer Tissues by MALDI Imaging Mass Spectrometry. J Proteome Res 9(4): 1854-1863.

36. Bauer JA, Chakravarthy AB, Rosenbluth JM, Mi D, Seeley EH, et al. (2010) Identification of markers of taxane sensitivity using proteomic and genomic analyses of prostate tumors from patients receiving neoadjuvant paclitaxel and radiation. Clin Cancer Res 16(2): 681–690.

37. Reyzer ML, Caldwell RL, Dugger TC, Forbes JT, Ritter CA, et al. (2004) Early changes in protein expression detected by mass spectrometry predict tumor response to molecular therapeutics. Cancer Res 64(24): 9093–9100.

38. Cazares LH, Troyer D, Mendrinos S, Lance RA, Nyalwidhe JO, et al. (2009) Imaging mass spectrometry of a specific fragment of mitogen-activated protein kinase/extracellular signal-regulated kinase kinase kinase 2 discriminates cancer from uninvolved prostate tissue. Clin Cancer Res 15(17): 5541–5551.

39. Lemaire R, Ait Menguellet S, Stauber J, Marchaudon V, Lucot J-P, et al. (2007) Specific MALDI Imaging and Profiling for Biomarker Hunting and Validation: Fragment of the 11S Proteasome Activator Complex, Reg Alpha Fragment, Is a New Potential Ovary Cancer Biomarker. Journal of Proteome Research 6(11): 4127–4134.

40. Patel SA, Barnes A, Loftus N, Martin R, Sloan P, et al. (2009) Imaging mass spectrometry using chemical inkjet printing reveals differential protein expression in human oral squamous cell carcinoma. Analyst. 134(2): 301–307.

41. Kang S, Shim HS, Lee JS, Kim DS, Kim HY, et al. (2010) Molecular proteomics imaging of tumor interfaces by mass spectrometry. J Proteome Res 9(2): 1157–1164.

42. Schwamborn K, Krieg RC, Reska M, Jakse G, Knuechel R, et al. (2007) Identifying prostate carcinoma by MALDI-Imaging. Int J Mol Med 20(2): 155–159.

43. Gustafsson JO, Oehler MK, McColl SR, Hoffmann P (2010) Citric acid antigen retrieval (CAAR) for tryptic peptide imaging directly on archived formalin-fixed paraffin-embedded tissue. J Proteome Res 9(9): 4315–4328.

44. Djidja MC, Claude E, Snel MF, Francese S, Scriven P, et al. (2010) Novel molecular tumour classification using MALDI-mass spectrometry imaging of tissue microarray. Anal Bioanal Chem 397(2): 587-601.

45. Cornett DS, Frappier SL, Caprioli RM (2008) MALDI-FTICR imaging mass spectrometry of drugs and metabolites in tissue. Anal Chem 80(14): 5648–5653.

46. Bouslimani A, Bec N, Glueckmann M, Hirtz C, Larroque C (2010) Matrix-assisted laser desorption/ionization imaging mass spectrometry of oxaliplatin derivatives in heated intraoperative chemotherapy (HIPEC)-like treated rat kidney. Rapid Commun Mass Spectrom 24(4): 415–421.

47. Trim PJ, Henson CM, Avery JL, McEwen A, Snel MF, et al. (2008) Matrix-assisted laser desorption/ionization-ion mobility separation-mass spectrometry imaging of vinblastine in whole body tissue sections. Anal Chem 80(22): 8628–8634.

How to cite this article: Rakesh S. New Approaches of Imaging MALDI, Protein Markers Part II: Prostate Cancer Drug Targeting Chemosensitivity Biosensors. Canc Therapy & Oncol Int J. 2021; 20(1): 556027. DOI: 10.19080/CTOIJ.2021.20.556027

48. Signor L, Varesio E, Staack RF, Starke V, Richter WF, et al. (2007) Analysis of erlotinib and its metabolites in rat tissue sections by MALDI quadrupole time-of-flight mass spectrometry. J Mass Spectrom 42(7): 900–909.

49. Hanselmann M, Kothe U, Kirchner M, Renard BY, Amstalden ER, et al. (2009) Toward Digital Staining using Imaging Mass Spectrometry and Random Forests. Journal of Proteome Research 8(7): 3558–3567.

50. Andersson M, Groseclose MR, Deutch AY, Caprioli RM (2008) Imaging mass spectrometry of proteins and peptides: 3D volume reconstruction. Nat Methods 5(1): 101–108.

51. Sinha TK, Khatib-Shahidi S, Yankeelov TE, Mapara K, Ehtesham M, et al. (2008) Integrating spatially resolved three-dimensional MALDI IMS with in vivo magnetic resonance imaging. Nat Meth 5(1): 57–59.

52. Grey AC, Chaurand P, Caprioli RM, Schey KL (2009) MALDI imaging mass spectrometry of integral membrane proteins from ocular lens and retinal tissue. J Proteome Res 8(7): 3278–3283.

53. Herring KD, Oppenheimer SR, Caprioli RM (2007) Direct tissue analysis by matrix-assisted laser desorption ionization mass spectrometry: application to kidney biology. Semin Nephrol 27(6): 597–608.

54. Aerni HR, Cornett DS, Caprioli RM (2006) Automated acoustic matrix deposition for MALDI sample preparation. Anal Chem 78(3): 827–834.

DOI:10.19080/CTOIJ.2021.20.556027

How to cite this article: Rakesh S. New Approaches of Imaging MALDI, Protein Markers Part II: Prostate Cancer Drug Targeting Chemosensitivity Biosensors. Canc Therapy & Oncol Int J. 2021; 20(1): 556027. DOI: 10.19080/CTOIJ.2021.20.556027